Electronic Supplementary Material (ESI) for ChemComm.

Dihydroartemisinin engages liver fatty acid binding protein and suppresses metastatic hepatocellular carcinoma growth

Mei-Ling Ruan,[abc] Yungen Liu,[d] Chunlei Zhang,[bc] Xiaowen Mao,[e] Di Hu,[bc] Chun-Nam Lok,[*bc] Judy Wai Ping Yam,[e] and Chi-Ming Che [*bcd]

[a] National Key Laboratory of Green Pesticide, College of Chemistry, Central China Normal University, Wuhan 430079, P. R. China

[b] State Key Laboratory of Synthetic Chemistry, and Department of Chemistry, The University of Hong Kong, Pokfulam Road, Hong Kong, P. R. China

[c] Laboratory for Synthetic Chemistry and Chemical Biology Limited, Hong Kong Science Park, Shatin, Hong Kong, P. R. China

[d] Department of Chemistry, Southern University of Science and Technology, Shenzhen, Guangdong, 518055, P. R. China

[e] Department of Pathology, The University of Hong Kong, Pokfulam Road, Hong Kong, P. R. China

*E-mail: cmche@hku.hk (Chi-Ming Che)
cnlok@hku.hk (Chun-Nam Lok)

Table of Contents

Experimental Procedures

Syntheses

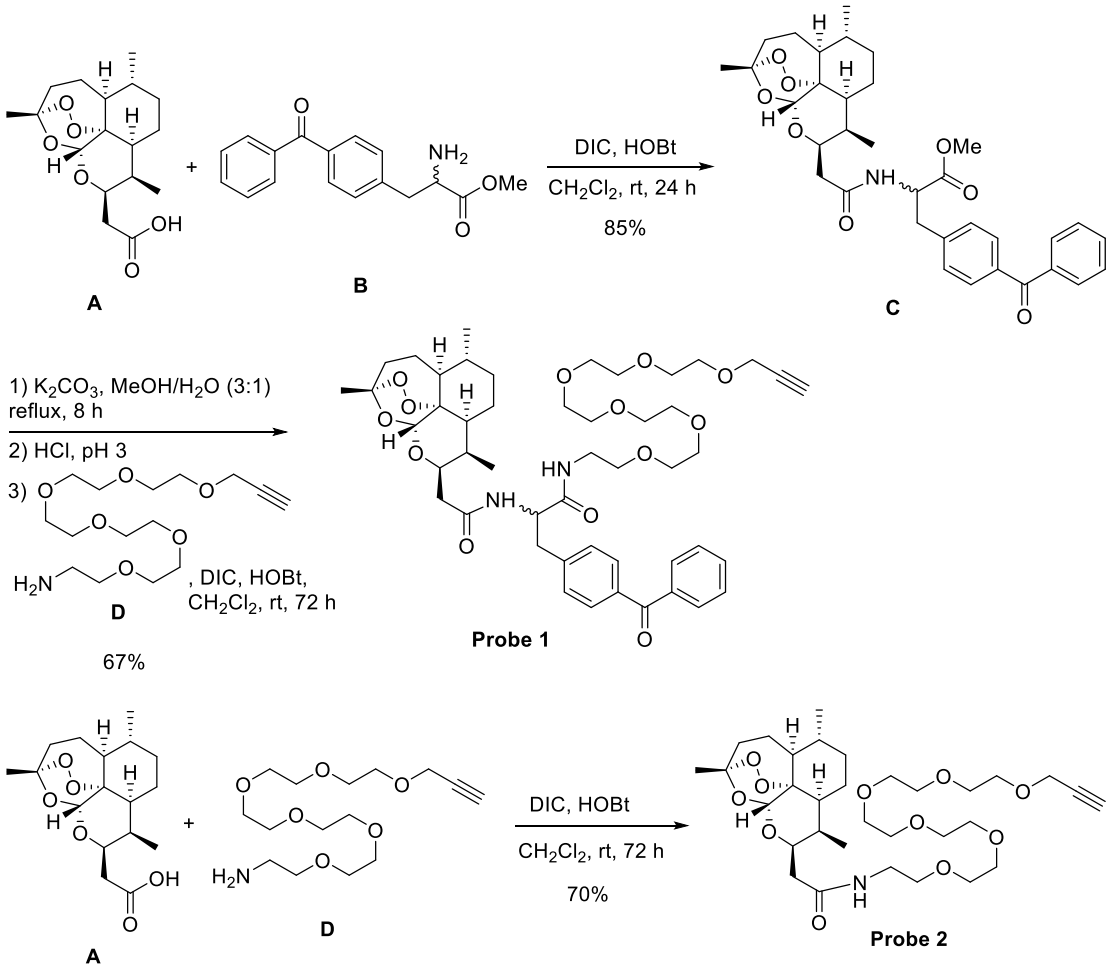

A was prepared according to the literature method[1].

B was prepared according to the literature method[2].

D was bought from Leyan® Chemical company in Shanghai, China.

Preparation of C.

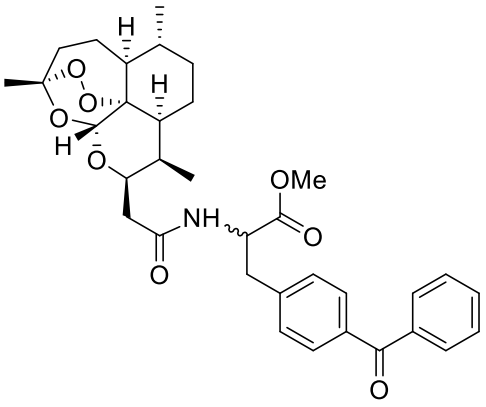

A mixture of **A** (326 mg, 1.0 mmol), **B** (racemic, 340 mg, 1.2 mmol), N,N'-diisopropylcarbodiimide (DIC, 0.3 mL, 2.0 mmol), N-hydroxybenzotriazole (HOBt, 27 mg, 0.2 mmol) in anhydrous dichloromethane (5 mL) was stirred for 24 h at room temperature under argon atmosphere. Then, the reaction mixture was concentrated under reduced pressure and the residue was purified by flash column chromatography on silica gel with hexane/ethyl acetate as eluent to afforded **C** in 85% yield (1:1 diastereomers).

^{1}H NMR (400 MHz, $CDCl_3$) (1:1 diastereomers) δ 7.81-7.73 (m, 4H), 7.62-7.56 (m, 1H), 7.51-7.45 (m, 2H), 7.39-7.31 (m, 2H), 5.38 (s, 1.5H), 5.34 (s, 1.5H), 4.95-4.70 (m, 2H), 4.57 (d, *J* = 8.0 Hz, 1H), 3.72 (s, 3H), 3.30-3.05 (m, 2H), 2.73-2.44 (m, 2H), 2.40-2.25 (m, 2H), 2.13-1.88 (m, 2H), 1.81-1.61 (m, 3H), 1.41 (s, 1.5H), 1.30 (s, 1.5H), 1.42-1.18 (m, 4H), 1.00-0.92 (m, 1H), 0.97 (d, J = 5.8 Hz, 1.5H), 0.96 (d, *J* = 5.8 Hz, 1.5H), 0.87 (d, *J* = 7.5 Hz, 1.5H), 0.85 (d, *J* = 7.5 Hz, 1.5H). ^{13}C NMR (101 MHz, $CDCl_3$) (1:1 diastereomers) δ 196.35, 196.30, 171.64, 171.48, 171.38, 171.17, 141.49, 141.22, 137.60, 137.55, 136.08, 136.06, 132.31, 132.23, 130.34, 130.26, 129.85, 129.42, 129.19, 128.24, 128.19, 128.17, 103.07, 103.02, 89.73, 89.27, 80.71, 80.63, 70.91, 69.62, 53.54, 53.30, 52.22, 51.90, 51.74, 43.76, 43.50, 37.72, 37.51, 37.39, 37.36, 37.22, 36.98, 36.45, 36.36, 34.17, 34.11, 30.07, 30.01, 25.69, 25.55, 24.67, 24.62, 24.58, 24.53, 19.97, 19.91, 12.64, 12.25.

Preparation of Probe 1.

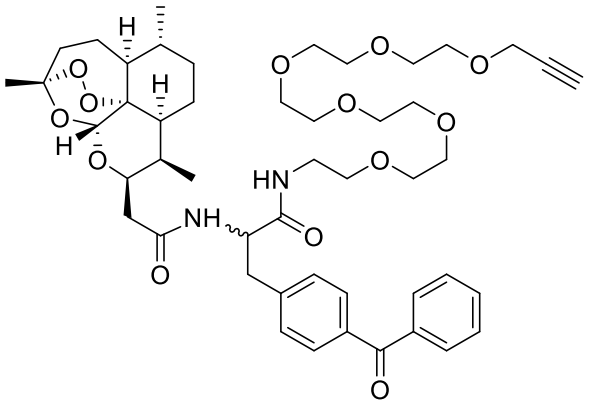

A mixture of **C** (296 mg 0.5 mmol) and K_2CO_3 (138 mg, 1.0 mmol) in 5 mL of MeOH/H_2O (v:v 3:1) was refluxed for 8 h. After cooling down to room temperature, the reaction mixture was washed with petroleum ether (discarded) and the aqueous solution was adjust pH to 3 by HCl. Then the aqueous fraction was extracted with dichloromethane (20 mL x 3). The combined dichloromethane fraction was dried over Na_2SO_4, filtered and concentrated under reduced pressure. The residue (acid) was used directly for next step with purification. A solution of acid (173 mg, 0.3 mmol), amine **D** (160 mg, 0.5 mmol), N,N'-diisopropylcarbodiimide (DIC, 75 mg, 0.6 mmol), N-hydroxybenzotriazole (HOBt, 14 mg, 0.1 mmol) in anhydrous dichloromethane (3 mL) was stirred for 72 h at room temperature under argon atmosphere. Then, the reaction mixture was concentrated under reduced pressure and the residue was purified by flash column chromatography on silica gel with dichloromethane/methanol as eluent to afforded **Probe 1** in 67% yield (1:1 diastereomers).

^{1}H NMR (400 MHz, $CDCl_3$) (1:1 diastereomers) δ 7.81-7.72 (m, 4H), 7.62-7.56 (m, 1H), 7.48 (t, *J* = 7.4 Hz, 2H), 7.38 (d, *J* = 7.4 Hz, 2H), 7.05 (t, *J* = 5.5 Hz, 1H), 5.38 (s, 1.5H), 5.34 (s, 1.5H), 4.81-4.66 (m, 2H),

4.19 (d, *J* = 2.4 Hz, 2H), 3.72-3.35 (m, 22H), 3.30-3.05 (m, 2H), 2.73-2.44 (m, 4H), 2.44 (t, *J* = 2.4 Hz, 1H), 2.36-2.25 (m, 2H), 2.10-1.88 (m, 2H), 1.81-1.60 (m, 3H), 1.44 (s, 1.5H), 1.37 (s, 1.5H), 1.42-1.18 (m, 4H), 1.00-0.92 (m, 1H), 0.96 (d, J = 5.5 Hz, 3H), 0.86 (d, *J* = 7.3 Hz, 1.5H), 0.84 (d, *J* = 7.3 Hz, 1.5H). ^{13}C NMR (101 MHz, $CDCl_3$) (1:1 diastereomers) δ 196.38, 171.63, 171.22, 170.60, 170.31, 142.50, 142.02, 138.08, 137.71, 137.65, 135.87, 132.28, 132.21, 130.30, 130.28, 129.90, 129.88, 129.52, 129.36, 129.33, 128.20, 103.13, 103.08, 89.82, 89.33, 80.74, 80.69, 79.61, 74.54, 70.94, 70.51, 70.48, 70.43, 70.40, 70.29, 70.18, 70.09, 69.81, 69.58, 69.55, 69.02, 58.31, 54.31, 54.15, 51.97, 51.77, 43.85, 43.49, 39.20, 38.25, 37.50, 37.41, 37.37, 36.49, 36.44, 34.24, 34.16, 30.09, 30.01, 25.83, 25.71, 24.72, 24.66, 24.62, 24.55, 20.02, 19.95, 12.68, 12.28. HR-MS (positive mode): calculated for $[M+H]^+$ 879.4638; $[M+NH_4]^+$ 896.4904; $[M+Na]^+$ 901.4458; Found $[M+H]^+$ 879.4636; $[M+NH_4]^+$ 896.4903; $[M+Na]^+$ 901.4457.

Preparation of Probe 2.

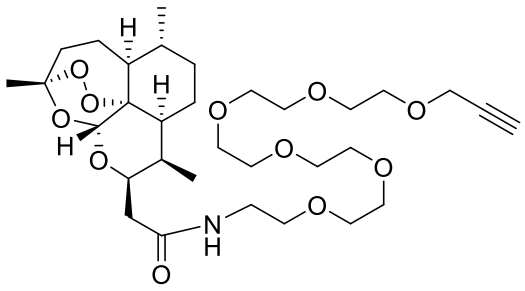

A solution of **A** (98 mg, 0.3 mmol), amine **D** (160 mg, 0.5 mmol), N,N'-diisopropylcarbodiimide (DIC, 75 mg, 0.6 mmol), N-hydroxybenzotriazole (HOBt, 14 mg, 0.1 mmol) in anhydrous dichloromethane (3 mL) was stirred for 72 h at room temperature under argon atmosphere. Then, the reaction mixture was concentrated under reduced pressure and the residue was purified by flash column chromatography on silica gel with dichloromethane/methanol as eluent to afforded **Probe 2** in 70% yield.

^{1}H NMR (400 MHz, $CDCl_3$) δ 7.08 (t, *J* = 5.8 Hz, 1H), 5.32 (s, 3H), 4.74-4.65 (m, 1H), 4.16 (d, *J* = 2.4 Hz, 2H), 3.69-3.55 (m, 22H), 3.52-3.30 (m, 2H), 2.62-2.44 (m, 2H), 2.41 (t, *J* = 2.4 Hz, 1H), 2.40-2.23 (m, 4H), 2.05-1.88 (m, 2H), 1.81-1.60 (m, 3H), 1.36 (s, 3H), 1.42-1.14 (m, 4H), 1.00-0.92 (m, 1H), 0.93 (d, J = 5.5 Hz, 3H), 0.83 (d, *J* = 7.3 Hz, 3H). ^{13}C NMR (101 MHz, $CDCl_3$) (1:1 diastereoisomers) δ 171.63, 102.92, 89.60, 80.76, 77.36, 77.04, 76.72, 74.52, 70.51, 70.49, 70.47, 70.44, 70.41, 70.37, 70.31, 70.21, 69.77, 69.02, 58.32, 51.87, 43.61, 39.23, 37.42, 37.28, 36.44, 34.22, 30.22, 25.80, 24.72, 24.66, 19.99, 12.31. HR-MS (positive mode): calculated for $[M+H]^+$ 628.3691; $[M+Na]^+$ 650.3511; Found $[M+H]^+$ 628.3685; $[M+Na]^+$ 650.3504.

Artemisinin compounds

Artemisinin (**ART,** ab141308) and Dihydroartemisinin (**DHA,** ab142690) were purchased from Abcam and the purity was verified by high resolution LC-MS and NMR analysis. They were freshly prepared in ethanol as 10 mM solution and used immediately before all experiments.

Cell culture

Hep G2 (human hepatocellular carcinoma) and PLC (human hepatocellular carcinoma) were obtained the American Type Culture Collection (ATCC). MHCC-97L (human hepatocellular carcinoma) were obtained from Cancer Institute, Fudan University, China. Hep G2, PLC and MHCC-97L were cultured in Dulbecco's Modified Eagle's Medium (DMEM) with fetal bovine serum (10%) and penicillin/streptomycin (100 U/mL, 1%) and maintained at 37 ℃ with 5% CO_2 (v/v).

Cell viability assay

The cytotoxicity of **ART**, **DHA**, **Probe 1** and **Probe 2** was evaluated by 3-(4,5-dimethylthiazol-2-yl)-2,5-diphenyltetrazolium bromide (MTT) assay. Cells were seeded in 96-well plates at ~ 5000/well and incubated overnight. All compounds were dissolved in ethanol. **ART** and **DHA** are freshly prepared. Media containing the tested complexes were added to the cells and serially diluted to various concentrations (i.e. from 100 μM to 0.2 μM). The maximum concentration of ethanol in media did not exceed 1 % (v/v). The cells were incubated for 72 h, followed by the addition of 10 μL of MTT solution (5 mg/mL) to each well and further incubation at 37 ℃ for 4 h. The formazan salt was solubilized by the addition of 100 μL of 10 % SDS solution. The cell survival as determined by absorbance of the colored solution at 590 nm was measured using a microplate reader (Varioskan™ LUX, ThermoFisher Scientific). The IC_{50} values were evaluated as the concentration at which 50 % of cell survival was inhibited.

Cell death assay

Hep G2 cells were seeded in 96-well plate at 4000 cells/well for 24 h at 37 ℃ and 5% CO_2 (v/v). Cells were treated with different concentrations of **DHA** for 72 h. Cells were stained with Hoechst 33342 (1 μM) and propidium iodide (1 μM) for 20 min at 37 ℃ for counting of total cells and dead cells, respectively. The cell imaging was performed with high content imaging system (Molecular Devices ImageXpress Micro Confocal) using DAPI (excitation at 405 nm, emission from 430-470 nm) and PE Texas Red channels (PI, excitation at 561 nm, emission from 580-595 nm) and brightfield imaging. Data were analyzed by MetaXpress software to obtain the total cell and dead cell counts.

Cell cycle analysis

Hep G2 cancer cells were treated with different concentrations of **DHA** for 48 h. Cells were then washed with PBS twice and detached by trypsinization. After centrifugation (1000 rpm, 5 min), cells

were fixed in cold ethanol (70%) for 30 min, centrifuged and resuspended in PBS containing RNase A (100 μg/mL) and propidium iodide (10 μg/mL). The fluorescence signals were manipulated with flow cytometry analysis (BD LSR Fortessa). 10,000 ungated events were acquired for each sample. Populations of cells at different phases of cell cycle were analyzed with FlowJo software.

Orthotopic HCC and lung metastasis model

BALB/cAnN-nu mice were orthotopically implanted with luciferase-labeled tumor seed derived from MHCC97L cells in liver. MHCC97L is a metastatic HCC cell line obtained from Cancer Institute, Fudan University, China. One week after implantation, mice were randomized into 2 groups with 7 mice each. Mice were treated with vehicle (10% (v/v) PET (PEG 60%, Ethanol 30%, Tween 80 10%) in PBS) and **DHA** (100 mg/kg, freshly prepared in 10 % PET in PBS before treatment) twice a week by intraperitoneal injection for a total of 8 weeks. For bioluminescence imaging of animals, mice were peritoneally injected by 100 μL D-luciferin (30 mg/ml) and imaged using IVIS spectrum imaging system (Perkin Elmer). Mice were then sacrifice and liver and lungs tissues were resected for bioluminescence imaging. Lung tissues were processed and stained with hematoxylin and eosin for histological analysis. Body weight of mice was measured weekly throughout the experimental period. The animal study was performed under the research protocol CULATR 5815-21 approved by the Committee of the Use of Live Animals in Teaching and Research (CULATR). The animal procedure was followed strictly according to the Animals (Control of Experiments) Ordinance (Hong Kong) and the guidance from Centre for Comparative Medical Research (CCMR), Li Ka Shing Faculty of Medicine, The University of Hong Kong.

Immunoblot analysis

Hep G2 cells (6×10^5 cells) were seeded in 6-well plate for 24 h and treated with **DHA.** Cells were washed with PBS for three times, and lysed with lysis buffer (200 μL, 50 mM Tris-HCl, pH 7.5, 150 mM NaCl, 10% glycerol, 1% Triton X-100, 0.1% SDS, 10 mM NaF, 5 mM sodium pyrophosphate, 5 mM sodium orthovanadate) with protease inhibitor cocktail on ice. The cell lysate was subjected to centrifugation at 15000 rpm, 4 ℃ for 15 min, and the cellular protein was quantified by the Bradford Protein Assay. 30 μg of protein samples were separated on a SDS-PAGE gel by electrophoresis and blotted on polyvinylidene fluoride (PVDF) membranes. The membrane was then blocked with 3% BSA in TBST buffer and incubated with corresponding primary antibodies at 4 ℃ overnight followed by appropriate secondary antibodies for further 2 h. The protein bands were visualized by the chemiluminescence procedure (ECL, GE healthcare). Equal loading of each lane was verified by GAPDH detection. The following primary antibodies were used: GAPDH from Cell Signaling Technology; FABP1 from Santa Cruz Biotechnology (sc-271591). The protein band signals on the blot images were quantified by Image J.

Cell treatment with probes, photo-affinity labelling and click reaction

Hep G2 cells were treated with **Probe 1** and **Probe 2** at 15 μM for 2 h. For competition assay with DHA, Hep G2 cells were treated with 10 μM **Probe 1** and **DHA** at ratio of 1:0, 1:3 and 1:10 (Probe 1: DHA) for 2 h. After replacing medium with PBS, photo-affinity reaction was performed by exposing the cells with ultraviolet irradiation at 365 nm using a UV lamp (Spectroline® ENF-280C) for 30 min on ice. Cells

were then lysed and clarified by centrifugation at 10,000 *g* at 4 ℃ The proteins in supernatant were isolated by acetone precipitation and dried by a SpeedVac Concentrator. Dried protein pellets were solubilized in 8 M urea in 100 mM Tris-HCl buffer (pH 7.4) and subjected to the click reactions in the presence of biotin-azide (100 μM) or fluorophore-azide (100 μM), tris(benzyltriazolylmethyl)amine (100 μM), $CuSO_4$ (1 mM) and sodium ascorbate (10 mM) for 2 h at room temperature.

Identification of photo-affinity-labelled targets of Probe 1 by 2-DE and MALDI-TOF MS

Hep G2 cells were treated with 20 μM of **Probe 1** or ethanol for 2 h followed by photo-affinity labeling, cell lysis and click reactions with Cy5-azide (100 μM, lumiprobe), tris(benzyltriazolylmethyl)amine (100 μM), $CuSO_4$ (1 mM) and sodium ascorbate (10 mM) for 2 h at room temperature. Proteins were then purified with acetone precipitation for overnight. The dried protein pellets were then solubilized in rehydration buffer (8 M urea, 4% CHAPS, 0.5% IPG buffer pH 3-10, 18 mM DTT and 0.002% bromophenol blue) and subjected to two dimensional gel electrophoresis (2-DE) according to previously reported protocol[2] using IPGphor Immobiline DryStrips (pH 3-10 NL, 13 cm, GE Healthcare) for the first dimension and 8% polyacrylamide gel for the second dimension. The gels were scanned for Cy5 fluorescence signals using Typhoon FLA9500 scanner (GE Healthcare) followed by silver staining for protein visualization. Protein spots of interest were excised, destained, dried and subjected to trypsin digestion (Trypsin Protease (Pierce, MS grade, 90057, ThermoFisher, 10 μg/mL in 25 mM NH_4HCO_3 buffer, pH 8.01, incubation at 37 ℃ for 45 min)[3]. The digested peptide samples were co-crystallized with α-cyano-4-hydroxycinnamic acid (CHCA) on the sample plate. The peptides were identified by Applied Biosciences 4800 MALDI-TOF/TOF MS. The combined MS and MS/MS data were searched against NCBInr database using MASCOT searching engine (Matrix Science).

Confirmation of FABP1 as the affinity-isolated protein of probe 1 by immunological analysis

Hep G2 cells were treated with 20 μM **Probe 1**, or vehicle for 2 h, and then subjected to UV cross-linking, cell lysis and click reactions with biotin-azide. The biotinylated proteins were isolated by Dynabeads® M-280 streptavidin beads (Thermo). After washing the beads with Wash Buffer I (50 mM Tris, pH 7.5, 150 mM NaCl, 10% glycerol and 1% Triton X-100), the captured proteins were eluted by incubation with 30 mM biotin and 5% SDS at room temperature for 15 min and then at 96 ℃ for 15 min. Proteins with or without the streptavidin affinity enrichment were separated by SDS-PAGE and subjected to immuno-blot analysis with streptavidin-horseradish peroxidase (Thermo), FABP1 (Santa Cruz Biotechnology) and GAPDH (Cell Signaling) antibodies.

Cellular thermal shift assay (CETSA) and isothermal dose-response assay (ITDRA)

For CETSA experiments, Hep G2 cells were seeded in 10 cm cell culture, grown overnight and treated with 20 μM **DHA** or 0.2 % ethanol for 2 h. Cells were washed with PBS and harvested by trysinization. Equal amounts of cell suspensions were aliquoted into PCR tubes and heated individually at different temperatures of 54-56 ℃, respectively, for 3 min followed by immediate cooling on ice. The cells were then lysed by 3 freeze-thaw cycles. The cell lysates were centrifuged at 100,000 × g for 20 min at 4 ℃ to pellet the denatured, precipitated proteins. The soluble proteins in the supernatant were analyzed by gel electrophoresis followed by immuno-blotting using FABP1 (Santa Cruz Biotechnology)

and Tubulin (Cell Signaling) antibodies. Isothermal dose response of stabilization of FABP1 by **DHA** was performed by exposing the cells or cell lysates to DHA at concentrations or ethanol vehicle for 2 h or 0.5 h, followed by heating the cells or cell lysates at 56 ℃ for 3 min. The cells were then lysed by 3 freeze-thaw cycles. The cell lysates were centrifuged at 100,000 × g for 20 min at 4 ℃ to pellet the denatured, precipitated proteins. The soluble proteins in the supernatants were analyzed by SDS-PAGE gel electrophoresis followed by immuno-blotting with FABP1 and GAPDH antibodies. The protein band signals on the blot images were quantified by Image J.

FABP1 siRNA transfection

FABP1 siRNA (121193) and negative control siRNA (No. 1) were purchased from Thermo (Silencer Select siRNA). Hep G2 cells were seeded into 6-well plates with a seeding density of 2×10^5 and incubated for 24 h. Then, siRNA and lipofectamine 2000 transfection reagent (Thermo) were added to 200 μL of Opti-MEM™ reduced serum medium (Gibco), mixed and incubated at room temperature for 20 minutes. Finally, the complex was added to the cells followed by incubation for 48 h. The FABP1 expression was measured by immunoblot.

Transactivation assay of PPARα

Hep G2 cells or PLC cells were seeded into 48-well plates at 0.4×10^5 cells per well and incubated for 24 h, followed by transfection with PPAR-responsive element driven luciferase reporter (PPREx3-TK-LUC, 0.1 μg, Addgene 1015), PPARα expression plasmid (0.025 μg, Addgene 22751) and PRL-TK plasmid (0.05 μg, Promega) for normalization of transfection efficiency. The negative control group was transfected with PPREx3-TK-LUC (0.1 μg), pcDNA 3.1 (+) (0.025 μg, Thermo) and PRL-TK (0.05 μg). The plasmids and 0.5 μL lipofectamine 2000 transfection reagent (Thermo) were added to 25 μL of serum-free medium (Opti-MEM™ reduced serum medium, Gibco), mixed and incubated at room temperature for 20 minutes. The complex was added to the cells followed by incubation for 24 h. Then, cells were treated with vehicle (ethanol), **DHA**, and PPARα agonist (GW7647 (Cayman), prepared in ethanol) for 24 h. The PPAR responsive reporter luciferase activities were assayed by Dual-Luciferase® Reporter Assay System (Promega) using a microplate reader (Varioskan™ LUX, Thermo).

Effects of FABP1 silencing and DHA on transactivation activity of PPAR

Hep G2 cancer cells were transfected with 100 nM FABP1 siRNA or negative control siRNA using lipofectamine 2000 transfection reagent (Thermo) for 24 h. Then, the siRNA transfected cells were further transfected with PPAR-responsive element driven luciferase reporter PPREx3-TK-LUC and PRL-TK for 24 h followed by treatment with vehicle (ethanol) and **DHA** (50, 100 μM) for another 24 h. The PPAR responsive reporter luciferase activities were assayed as aforementioned.

Effects of FABP1 silencing and DHA on Hep G2 cell viability

Hep G2 cancer cells were transfected with 100 nM FABP1 siRNA or negative control siRNA using lipofectamine 2000 transfection reagent (Thermo) for 24 h. Then, the siRNA transfected cells were

treated with different concentrations of **DHA** (freshly prepared in ethanol) for 48 h. Cell viability was measured by MTT assay.

Statistical Analysis

The statistical differences were analyzed using the Student's t-test and considered significant when P< 0.05.

Protein purification

Human FABP1 with a N-terminal His-tag was expressed using FABP1 sequence (NM_001433) cloned into pET28a(+) plasmid (Genscript). [4] BL21(DE3) *E.coli* transformed with the plasmid was grew overnight at 25 °C in the presence of 0.2 mM isopropyl-β-D-1-thio-galactopyranoside (IPTG). 1 L of bacteria was pelleted and resuspended in 25 ml of lysis buffer (20 mM Hepes, 300 mM NaCl, 10 mM imidazole, pH 7.4, supplemented with protease inhibitor cocktail and 10 μg/mL PMSF. After sonication (four cycles, with pulses lasting 20 s/cycle, and with 1 min interval between cycles to prevent heating), lysates were centrifuged at 12,000 × g for 20 min at 4 °C. Solubilized proteins were affinity purified on Ni-NTA Agarose beads (Thermo scientific) and eluted with lysis buffer supplemented with 300 mM imidazole. Finally, buffer exchange of the proteins against 20 mM Hepes, 100 mM NaCl, 5 % glycerol, pH 7.4 were performed using dialysis membrane (Sigma-Aldrich). His-FABP1 was incubated with thrombin for 4 h, then purified on Ni-NTA Agarose beads (Thermo scientific), and further purified by Fast protein liquid chromatography (FPLC, Cytiva). Protein samples were aliquoted and stored at −80 °C.

Surface Plasmon Resonance (SPR) binding study

The binding affinity between **DHA** (freshly prepared in DMSO) and FABP1 was measured using an Biacore T200 instrument (Cytiva) by Nantong Hujia Biotechnology Co Ltd. as previously described.[5] Briefly, Protein FABP1 was immobilized on the surface of CM5 chip by using amine-coupling approach at a flow rate of 10 μL/min in 10 mM sodium acetate buffer (pH 5.5). The sensor surface was activated with a 7 min injection of the mixture of 50 mM N-hydroxysuccinimide (NHS) and 200 mM 1-ethyl-3-(3-dimethylaminopropyl) carbodiimide (EDC). Then 10 μg/mL of FABP1 was injected and the surface was blocked with 1 M ethanolamine, pH 8.5. Series concentrations of **DHA** were injected into the flow system and analyzed for 90 s, and the dissociation was 120 s. All binding analysis was performed at 25 °C in 20 mM HEPES, 100 mM NaCl buffer with 1% DMSO and 0.05% Tween-20, pH 7.4. Prior to analysis, double reference subtractions and solvent corrections were made to eliminate bulk refractive index changes, injection noise, and data drift. The binding affinity was determined by fitting to a Langmuir 1:1 binding model within the Biacore Evaluation software (Cytiva).

Isothermal Titration Calorimetry (ITC) binding study

The binding affinity between **DHA** and FABP1 was measured using MicroCal^{TM} PEAQ-ITC instrument (Malvern). The FABP1 protein (20 μM) in aqueous buffer (20 mM HEPES, 100 mM NaCl, 0.5% glycerol, pH 7.4) containing 5% ethanol was titrated against increasing concentrations of **DHA** (0-200 μM) and

heat released from each addition was recorded and the data of heat changes throughout the titration were fitted by using a non-linear least square method. Heat released from buffer control is negligible. The binding association constant (*K*) of the biomolecular interactions was obtained from the best-fitted graph. The apparent binding dissociation constant, K_d, is the inverse of *K*.

Micro-Scale Thermophoresis (MST) binding study

The binding affinity between **DHA** and FABP1 or PPARα was measured using an MST NT.115 instrument (Nano Temper). His-PPARα proteins were purchased from Cayman, lyophilized in 50 mM NaH_2PO_4, 100 mM NaCl, 20 % glycerol, pH 7.2. 10 μg of purified proteins was labeled with 0.15 μM Alexa Fluor® 647 (Thermo) according to the manufacturer's protocol. The labelled protein was mixed with different concentrations of **DHA** (0.0006-20 μM) followed by equilibration in a running buffer (20 mM Hepes, 100 mM NaCl, 0.05% Tween-20, pH 7.4) and MST analysis. The K_d values of **DHA** was determined using MO.Affinity Analysis software.

Remarks on SPR, ITC and MST for binding affinity measurement

SPR, ITC and MST are employed as alternative techniques for verifying the binding strength between DHA and FABP1. The deviation of the K_d determined by SPR, ITC and MST, apart from intrinsic detection properties, may be due to difference in binding environment being in protein immobilized state in SPR and in solution form in MST and ITC. SPR and ITC are label-free methods while our MST format requires fluorescent labelling of the proteins.

Computational methods

1. Parameterization of ligands

   Ligand molecules were first subject to geometry optimization at HF/6-31G* level and then the electrostatic potentials around the atoms were calculated by the MK method at the same QM level. QM calculations were performed using Gaussian09 [6]. With the help of antechamber in AmberTools [7], RESP atomic charges [8] and GAFF parameters [9] were calculated for the ligands.

2. Docking

   AutoDock (version 4.2.6) was chosen for the ligand-protein docking and AutoDockTools was used to prepare input files for docking [10]. The NMR ensemble of the holo-FABP1 bound by oleic acid (PDB code: 2L68) [11] was chosen and each conformer in the ensemble was extracted for docking. A grid box of 60 x 80 x 60 grids was defined at the center of the protein. For each conformer of FABP1, 100 GA runs were performed and the generated 100 binding poses of the ligand were subject to structural clustering with a cutoff of 2.0 Å for the cluster radius. The top three clusters ranked by their best scored binding poses were chosen for analysis.

3. MD simulations to assess the binding poses

MD simulations were performed using Gromacs, version 5.1.4 [12,13]. The complexes of FABP1-**DHA** were solvated in a cubic box with the minimum distance between the complex and walls of the box set to 1.0 nm. The Amber99SBildn force field [14] was used for protein. GAFF force field was used for the ligand. The TIP3P water model was used to model water molecules. Sodium chloride was added to 100 mM to neutral the system. The systems were simulated in the NPT ensemble, with the temperature set to 298.15 K and pressure set to 1.0 bar. The temperature and pressure were controlled by v-rescale[15] and Parrinello-Rahman methods [16], respectively. PME method was used to calculate electrostatic interactions with a cutoff set to 1.0 nm. The van der Waals interactions were evaluated by the cutoff method and the cutoff was set to 1.0 nm, as well. For each pose, the production run was 100-200ns.

Supplementary Figures

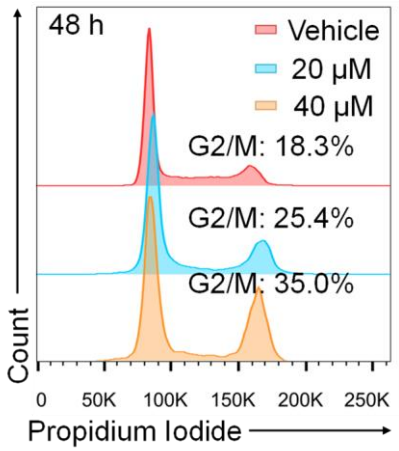

Fig. S1 Flow cytometric analysis of cell cycle distribution of Hep G2 liver cancer cells treated with **DHA** (20 or 40 μM) for 48 h.

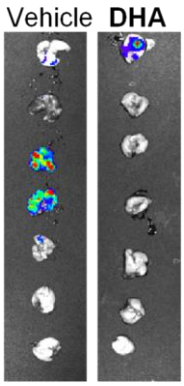

	Incidence of metastasis
Vehicle	4
DHA	1

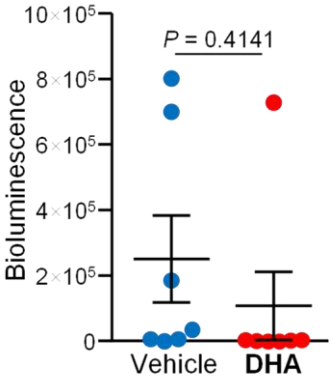

Fig. S2 Ex vivo bioluminescence imaging of dissected lung (left) and plot of luciferase signal (right). Incidence of lung metastasis is shown (middle).

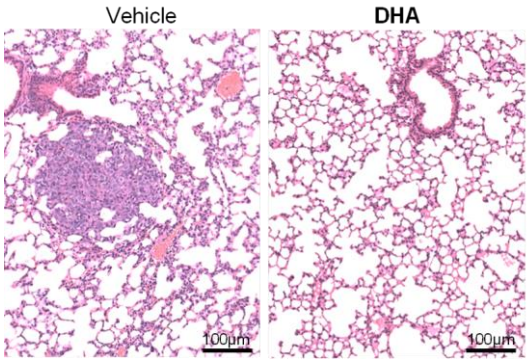

Fig. S3 Representative images of H&E staining of lung tissues after fixation. Scale, 100 μm.

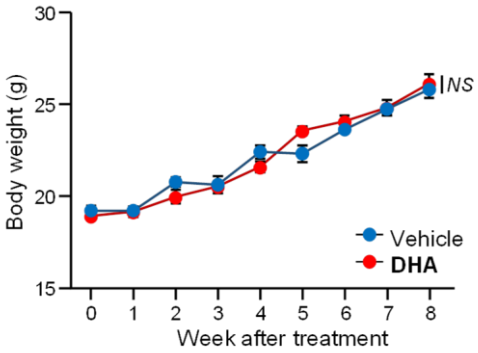

Fig. S4 Body weight was measured weekly. Data are presented as mean ± SEM. P < 0.05 is regarded as statistically significant. NS, not significant.

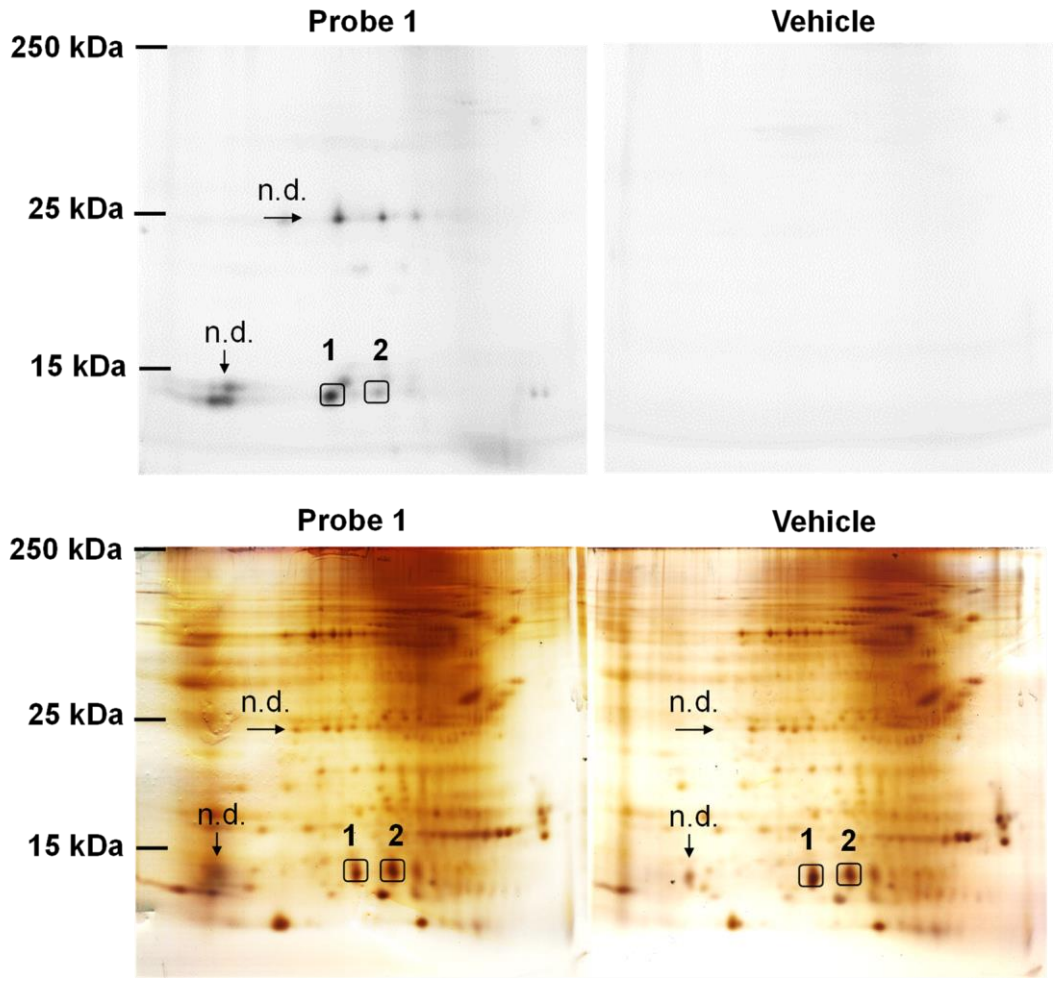

Fig. S5 Isoformic protein spots labeled with Cy5 on a 2D gel were identified as FABP1 by MALDI-TOF/TOF/MS. Hep G2 cells were incubated with **Probe 1** or Vehicle followed by irradiation and click reaction with Cy5-azide. The proteins were resolved on 2D gels and fluorescent Cy5 signals were detected by Typhoon scanner followed by silver staining of the gels. Spot 1-2: the proteins colocalized with Cy5 signals were identified as FABP1 by MALDI-TOF/TOF MS (Fig. 4C & Table S1). n.d., unidentified.

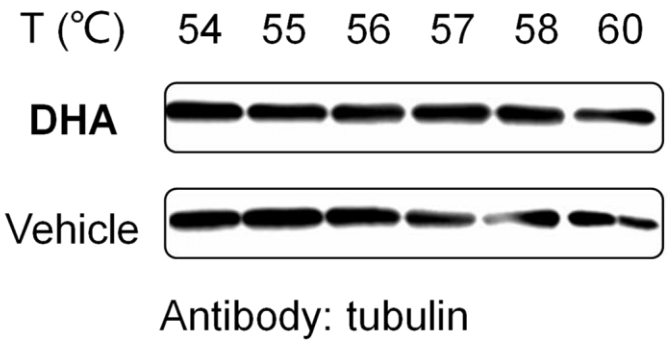

Fig. S6 (Supplementary data of Fig. 5A, Engagement of FABP1 by **DHA** in Hep G2 cells). Cellular thermal shift assays with immunoblot detection of tubulin in Hep G2 cells.

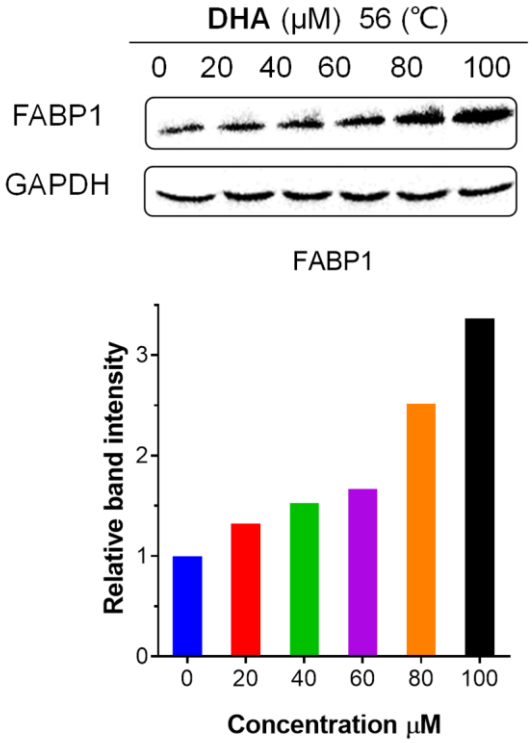

Fig. S7 Immunoblots from isothermal (56 ℃) dose response assays on Hep G2 cell lysates treated with increasing concentrations of **DHA**.

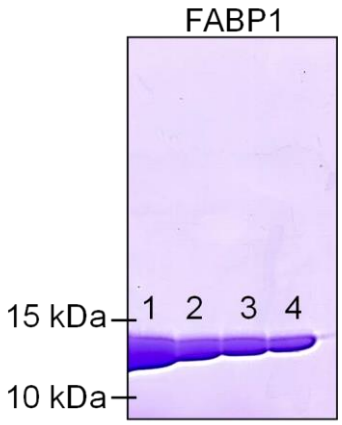

Fig. S8 Purified FABP1 (~ 14 kDa). Lane 1-4, Coomassie Brilliant Blue staining of the purified protein eluted by fast-protein liquid chromatography (FPLC).

Molecular Docking and Molecular Dynamic Simulations

To all 20 conformers, the best binding energy was estimated at -6.28 kcal/mol. To the same conformer of FABP1, the second and third clusters of **DHA** binding poses displayed binding energies of -5.26 kcal/mol and -5.21 kcal/mol, respectively. Visual inspection to these three clusters revealed that these three binding poses of **DHA** occupied three binding sites, respectively (denoted as P1, P2, P3 in Fig. S9). The binding site P1 is located at the entrance to the hollow pocket of FABP1, while the second site P2 is located near the conserved R122. P3 is the deepest site flanked by two phenylalanine residues F50 and F95.

These three binding poses were then subject to 100ns MD simulations to assess their stabilities. All three binding poses experienced large rearrangements (Fig. S10) after the MD simulations and the largest change occurred to the first pose with the largest ligand rmsd (>12 Å). Since the NMR structure of FABP1 used here was that bound by oleic acid molecules [10], it is not surprising to observe large rearrangements of the ligand binding poses after MD relaxation, and it is possible for **DHA** to achieve better interactions with FABP1. Therefore, these MD relaxed binding poses were re-evaluated and the new binding energies were -3.51 kcal/mol, -4.07 kcal/mol and -5.63 kcal/mol for P1, 2 and P3, respectively. This observation is interesting because the binding energies of these relaxed binding poses decrease as **DHA** goes deeper in the hollow pocket of FABP1, which is the reverse trend of the original docking results. Since the binding sites P1 and P2 are at or close to the entrance of the hollow pocket, it is reasonable to hypothesize these two sites as the transient binding sites. Through these two sites, **DHA** goes deeper to the P3 site and adopts better interactions. Consistently, extending MD simulation of the third pose to 200 ns lead to a better binding energy as -6.33 kcal/mol.

P3 accommodates the hydrophobic alkyl chain of oleic acid or the N-cyclohexyl urea moiety of GW7647. **DHA** overlaps with these two ligands as shown in Fig. 5E&F in the main text. Particularly, the orientation of **DHA** is similar with the N-cyclohexyl urea moiety of GW7647 (Fig. 5F), probably due to the similar amphiphilic character of their molecular surfaces. Figure S7 shows the interaction details between **DHA** and FABP1. The hydrophilic surface of **DHA** faces hydrophilic residues of the protein and a number of hydrogen bonds formed between **DHA** and residue of T73, T93, S100 and N111. The other side of the molecule, however, faces hydrophobic packet formed by I41, F50, F63 and L91. The phenyl ring of F50 forms close contacts with the cyclohexane ring of **DHA**. Therefore, it is quite possible for this molecule to bind to P3.

We also noticed the discrepancy between our predicted binding energy (-6.33 kcal/mol) at P3 and that obtained from ITC (-8.01 kcal/mol). The issue is due to the fact that **DHA** binding to FABP1 is entropy driven ($T\Delta S$ = 5.85 kcal/mol). If **DHA** as expected binds to the deeply buried P3 site, it displaces water molecules, which is entropically favorable. However, AutoDock cannot capture such effect due to the intrinsic limitations in its score function [17]. Therefore, it is understandable to obtain a weak binding affinity estimation by AutoDock.

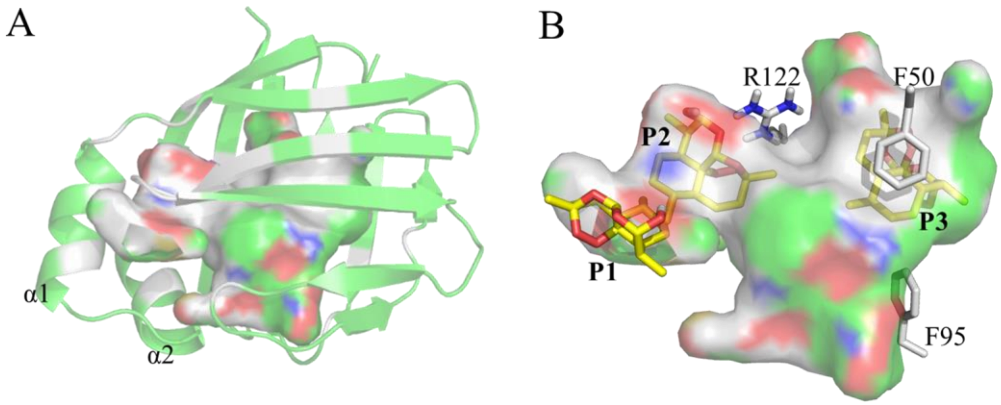

Fig. S9 Structure of FAPB1 and the binding poses of **DHA** in the hollow pocket of FABP1. (A) The second conformer of the NMR ensemble (PDB code 2L68) of holo-FABP1 bound by oleic acid. The hollow pocket is shown by surface. The two α-helices forming the gate of the entrance to the hollow entrance are labeled. (B) The predicted by docking predicted binding sites (P1, P2 and P3) of **DHA** in the hollow pocket. **DHA** are depicted as stick models with carbon atoms colored in yellow. Key amino acids are labeled.

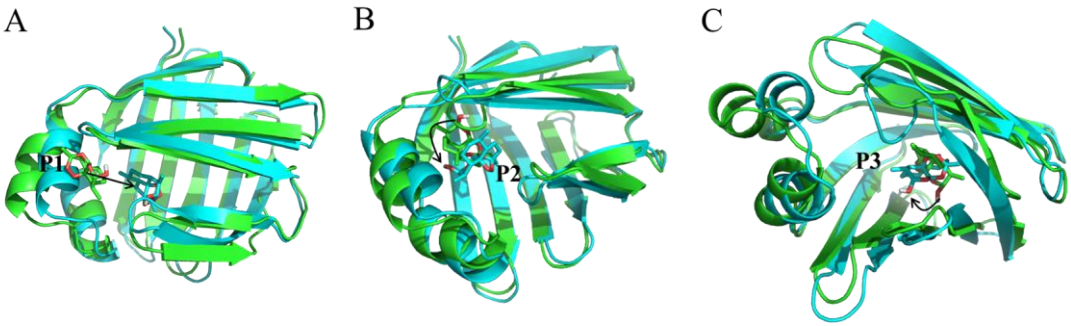

Fig. S10 Structural changes of **DHA**-FABP1 complexes after 100 ns MD simulations. (A), (B) and (C) are complexes of **DHA** at P1, P2, P3 sites, respectively. The initial structures are colored in green, while the MD 100ns structures are colored in cyan. **DHA** molecules are represented by sticks. The movement of **DHA** is indicated by black arrows.

The binding energy of **ART** to FABP1 was estimated at -5.14 kcal/mol and the dissociation constant is 171.1 μM which is about 7.5 folds weaker than **DHA**. as shown in Fig. S11, Structural comparison between the complexes of **ART**/FABP1 and **DHA**/FABP1 revealed significant differences in atomic interactions. There are only three hydrogen (H) bonds formed between **ART** and FABP1, which involve the three oxygen atoms of the lactone moiety of **ART** and the hydroxyl groups of residues T93 and S100. The H bonds between the peroxide oxygen atoms of **DHA** and side chains of T73 are not observed for **ART**, which is due to the rotation of T73 side chain. In addition, the H bond between the side chain amide of N111 and the hydroxyl oxygen of **DHA** is also missing, and the side chain amide group of N111 moves away from **ART**. Therefore, the weaker affinity of **ART** to FABP1 is mainly due to the loss of these H bonds. The structural difference between **ART** and **DHA** is associated with the reduction of the carbonyl group of **ART** to the hydroxyl group of **DHA**. This chemical modification increases the volume, changes the stereo configuration and the capacity of H bond formation of this functional group. OH group can be both an H bond donor and acceptor, while the C=O oxygen can only be an H bond acceptor. For **DHA**, the OH group acts as an H bond donor to bind the hydroxyl group of S100. For **ART**, the carbonyl oxygen can only act as an H bond acceptor to bind the hydroxyl group of S100. As a result, the side chain of S100 rotates by around 180˚ and pushes the side chain of N111 away from the carbonyl group of **ART**. In the meantime, the whole molecule of **ART** rotates a little bit, missing the H bonds between the peroxide bridge and the side chain of T73.

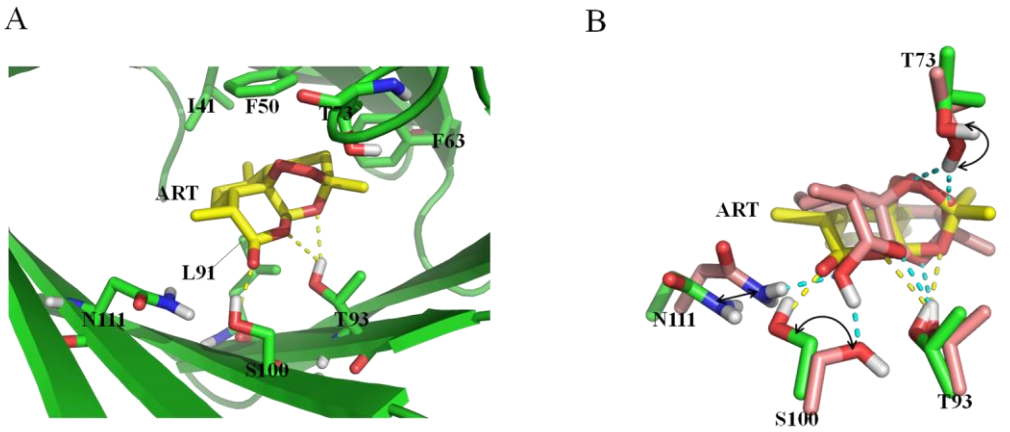

Fig. S11 (A) **ART** binding pose in FABP1. Residues around **ART** are depicted by sticks. The hydroxyl groups of T93 and S100 form hydrogen bonds (dashed yellow lines) with the three oxygen atoms of the lactone moiety. (B) Comparison of binding poses of **ART** (yellow carbons) and **DHA** (pink carbons). The FABP1 proteins are superimposed. FABP1 bound by **ART** is coloured in green for carbon atoms, while FABP1 bound by **DHA** is coloured in pink for carbons. The dashed yellow lines represent hydrogen bonds between **ART** and FABP1, while dashed cyan lines show the hydrogen bonds between **DHA** and FABP1. Black arrows indicate the rotamer difference of side chains of residues.

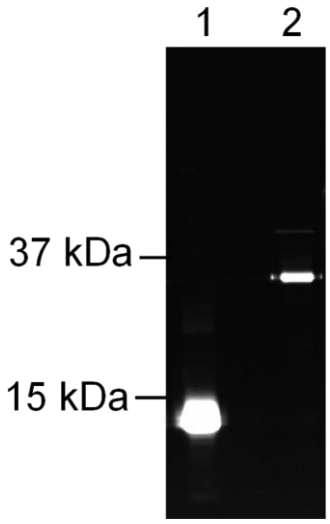

Fig. S12 FABP1 (~ 14 kDa) and PPARα (~ 34 kDa) were labelled using Alexa Fluor® 647 NHS Ester followed by SDS-PAGE to detect the labelled proteins (Line 1: FABP1, Line 2: PPARα).

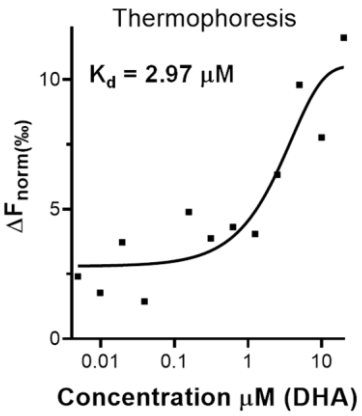

Fig. S13 Microscale thermophoresis measurement of the binding affinity of **DHA** with FABP1.

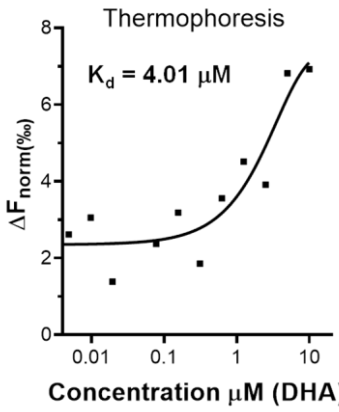

Fig. S14 Microscale thermophoresis measurement of the binding affinity of **DHA** with PPARα.

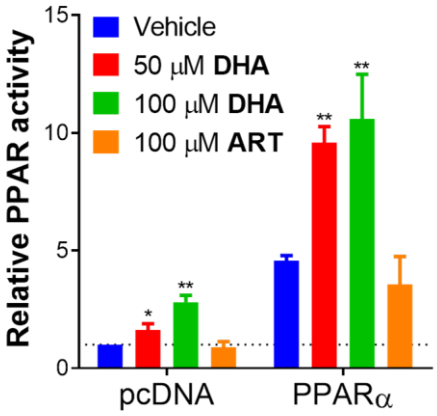

Fig. S15 PPARα transcriptional activation by **ART** in Hep G2 cells. Concentration dependence of transcriptional activation of PPARα in Hep G2 cells treated with **ART**, **DHA** and vehicle alone for 24 h. The effect of drugs on PPARα activity was expressed relative to vehicle-treated control. Data shown are mean value ± S.D. from three independent experiment. *P < 0.05; **P < 0.01 versus untreated control group.

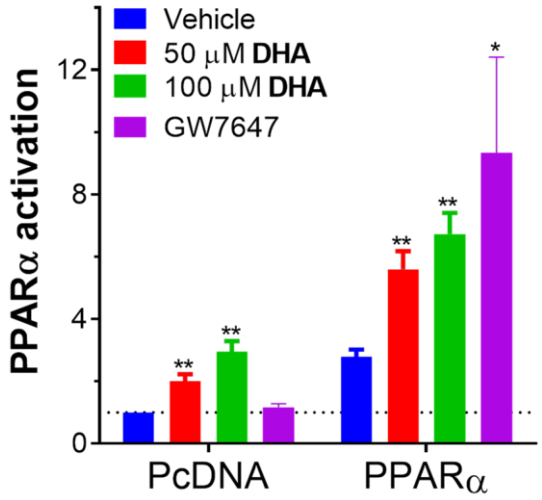

Fig. S16 PPARα transcriptional activation by **DHA** in PLC cells. Concentration dependence of transcriptional activation of PPARα in PLC cells treated with **DHA**, PPARα agonists (GW7647, 6 μM) and vehicle alone for 24 h. The effect of drugs on PPARα activity was expressed relative to vehicle-treated control. Data shown are mean value ± S.D. from three independent experiment. *P < 0.05; **P < 0.01 versus untreated control group.

^{1} H NMR and ^{13} C NMR spectra

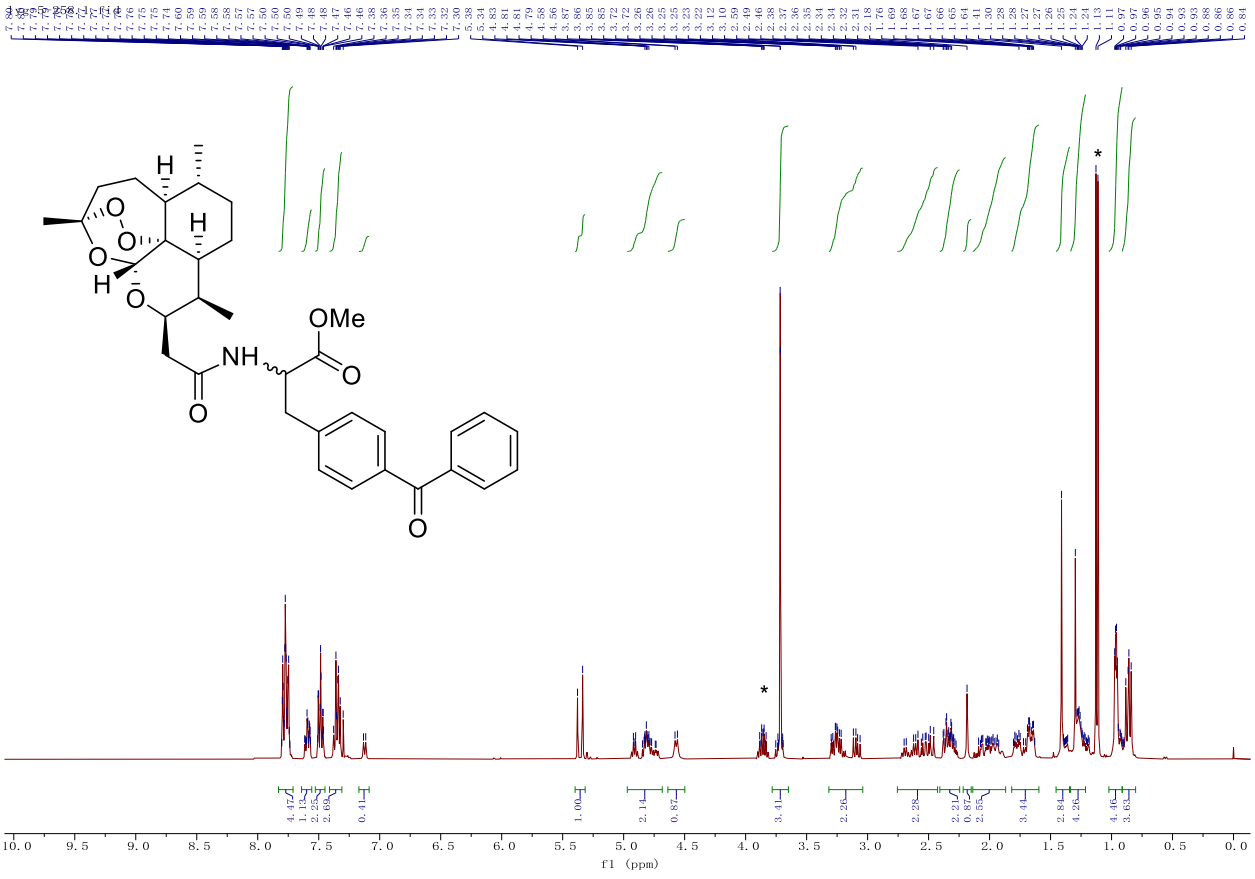

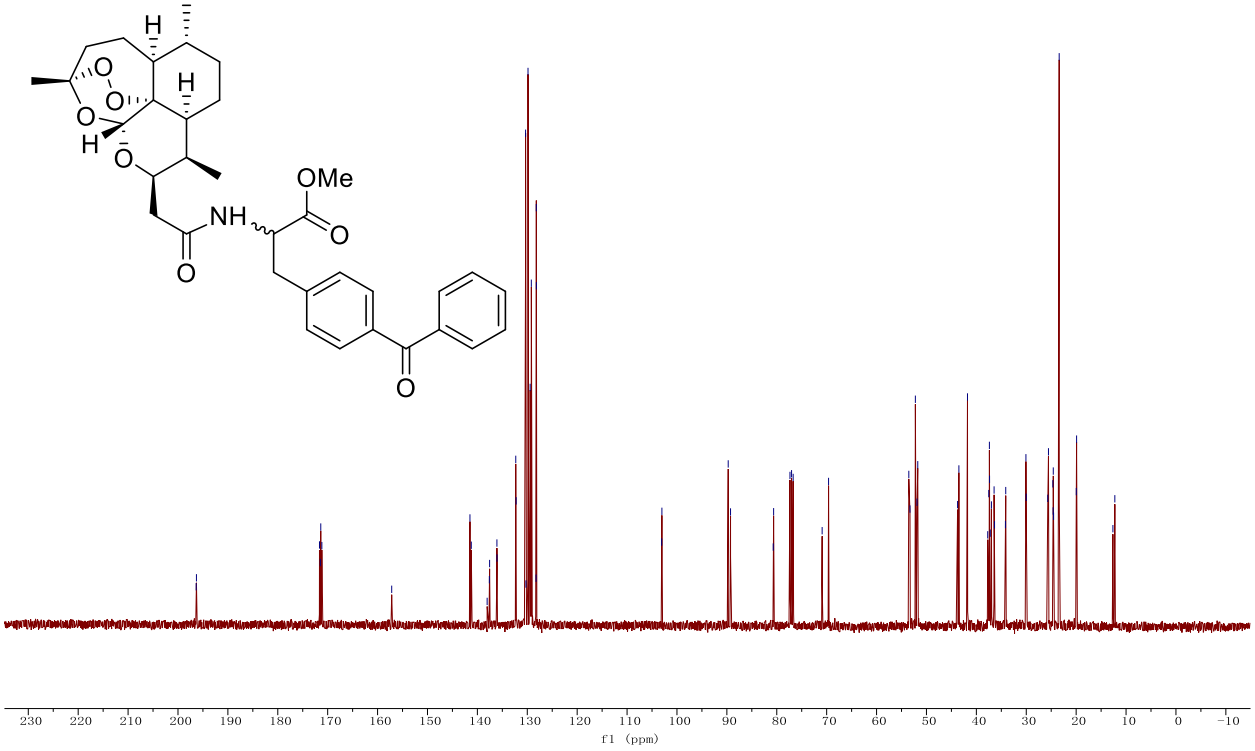

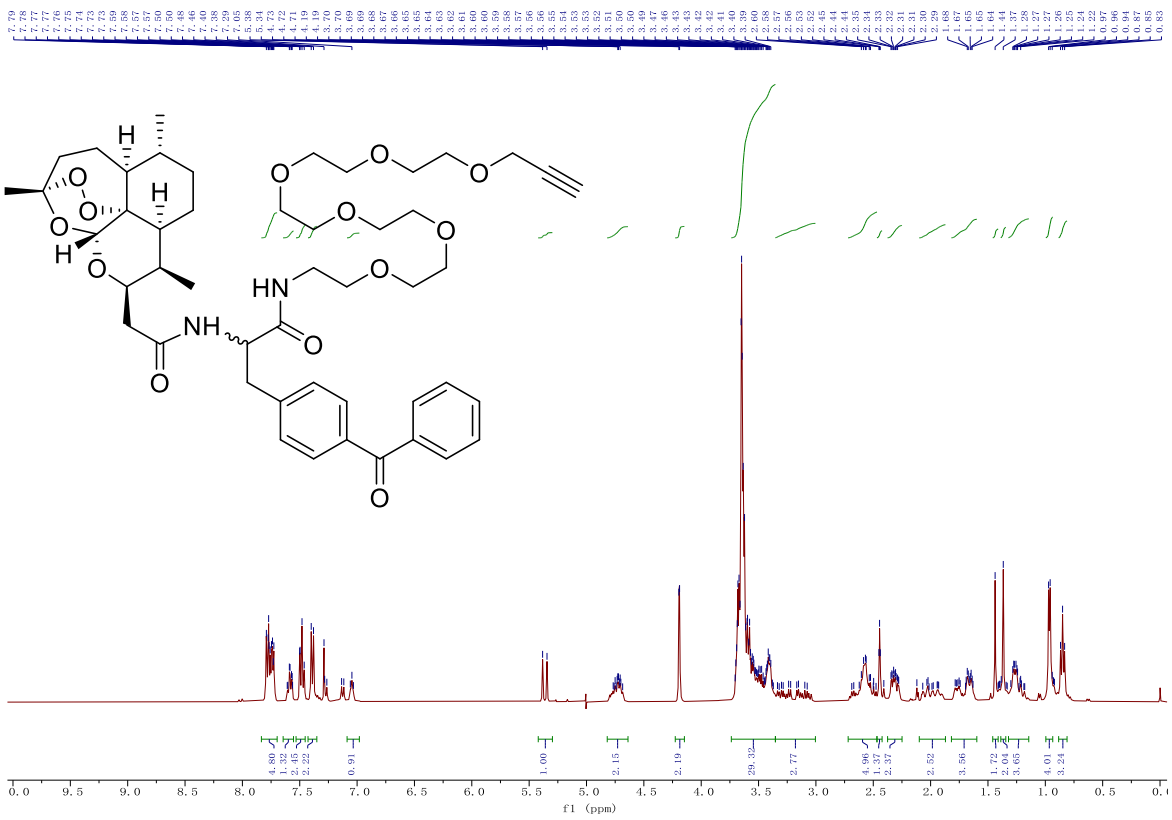
f1 (ppm)

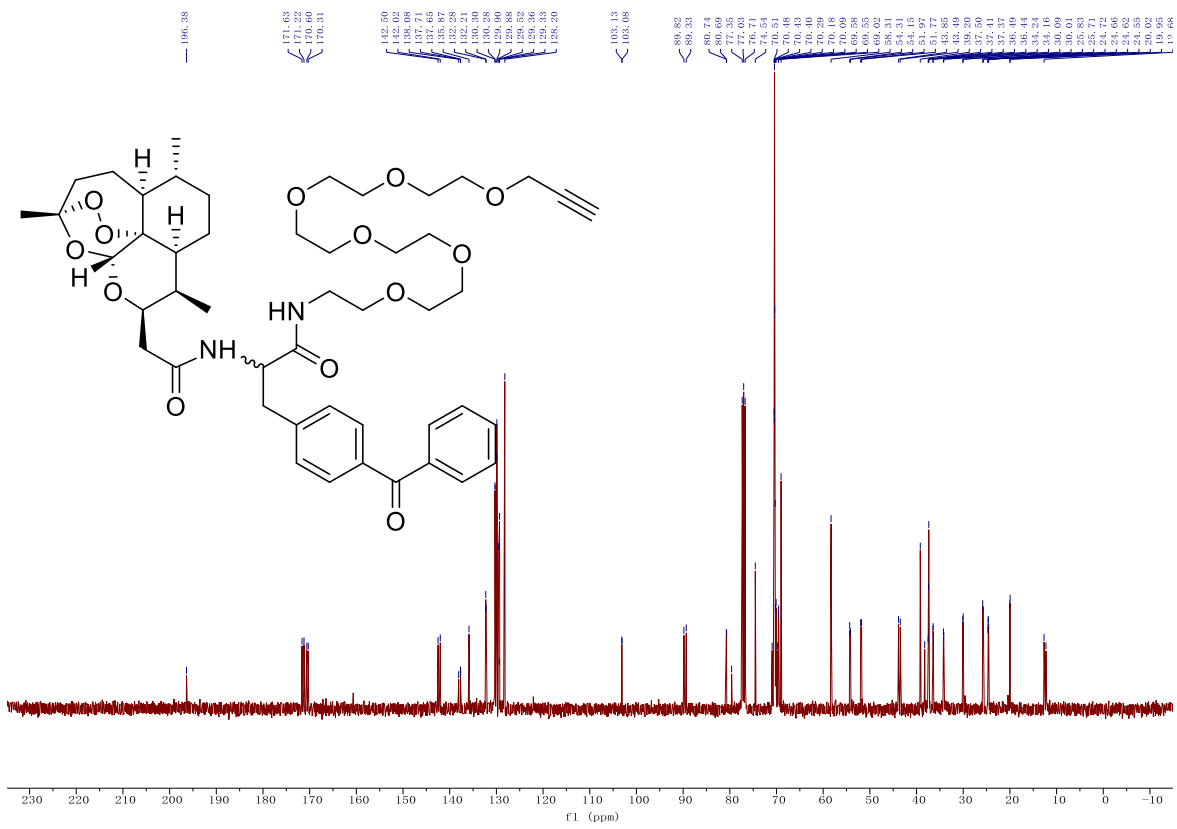
f1 (ppm)

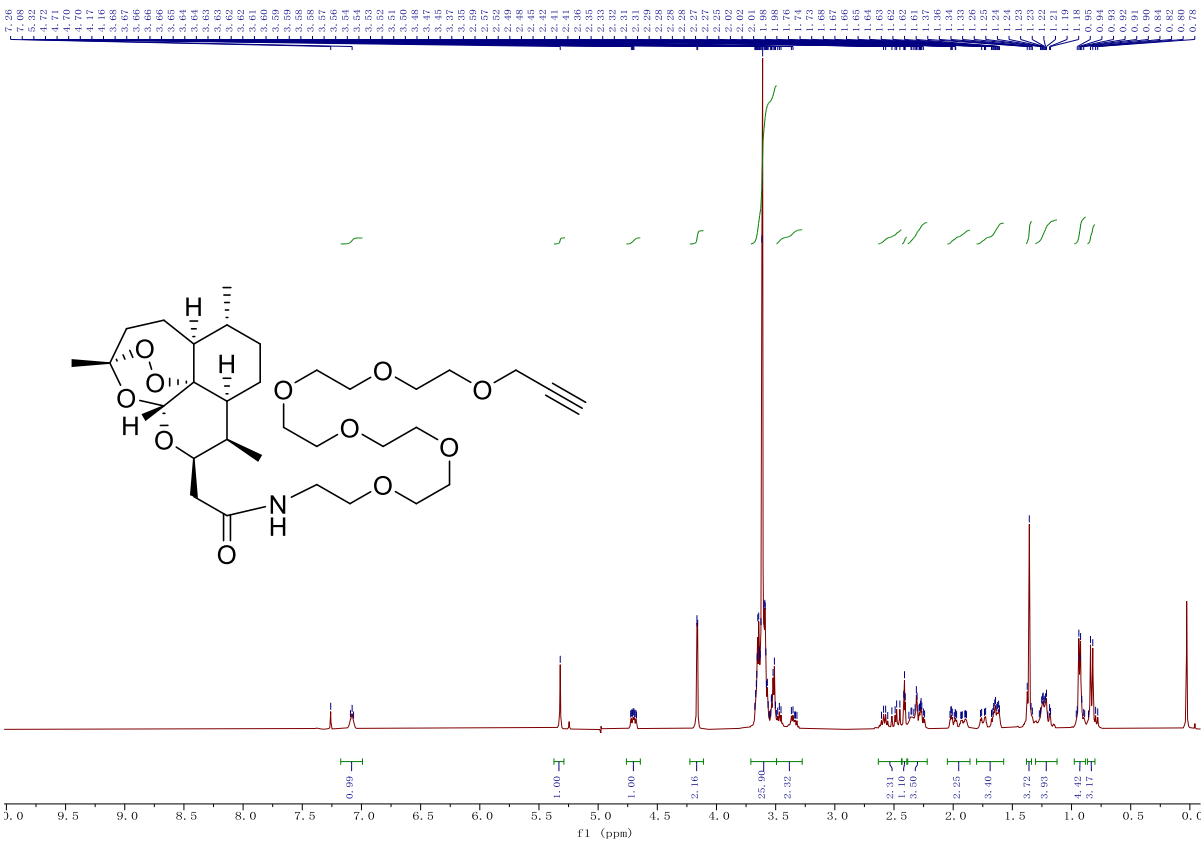
f1 (ppm)

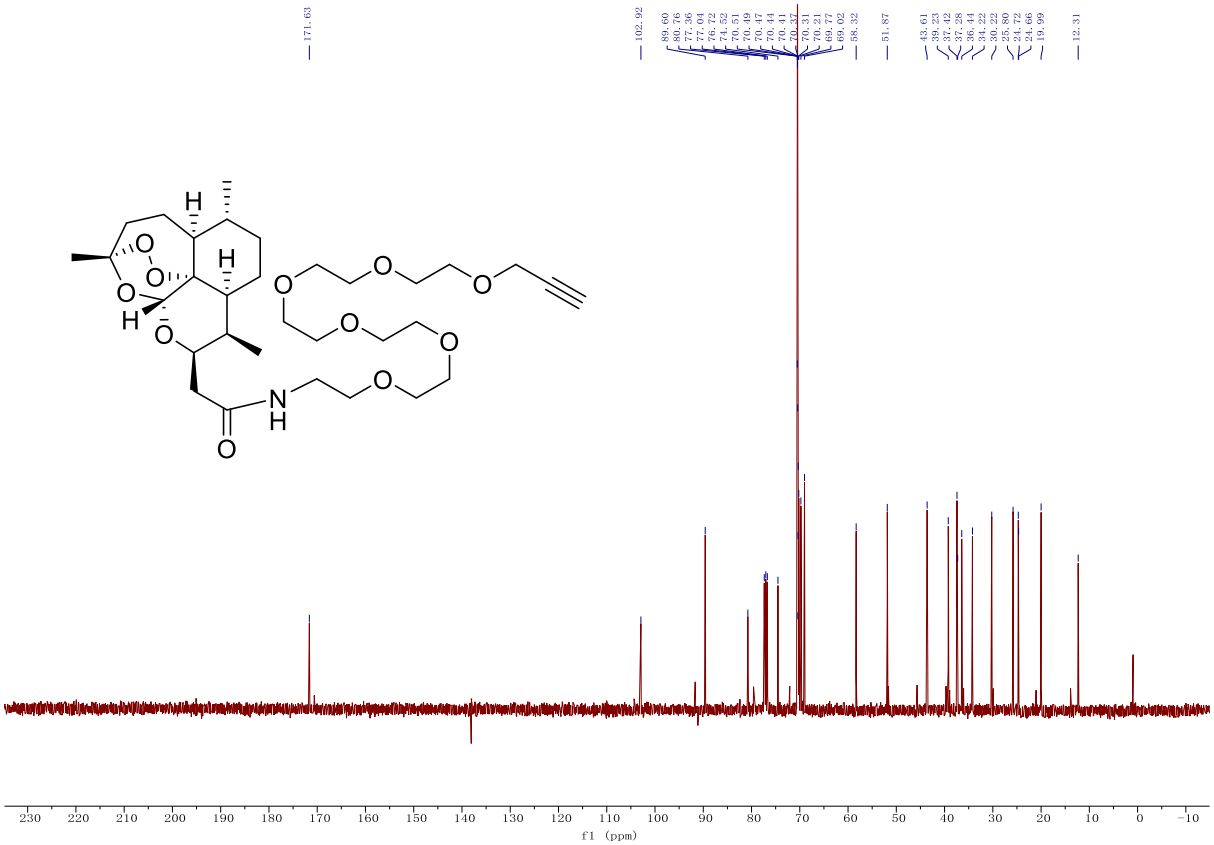
f1 (ppm)

High Resolution-Mass spectra (HR-MS) by Q-TOF Mass Spectrometry.

Probe 1: HR-MS (positive mode): calculated for $[M+H]^+$ 879.4638; $[M+NH_4]^+$ 896.4904; $[M+Na]^+$ 901.4458; Found $[M+H]^+$ 879.4636; $[M+NH_4]^+$ 896.4903; $[M+Na]^+$ 901.4457.

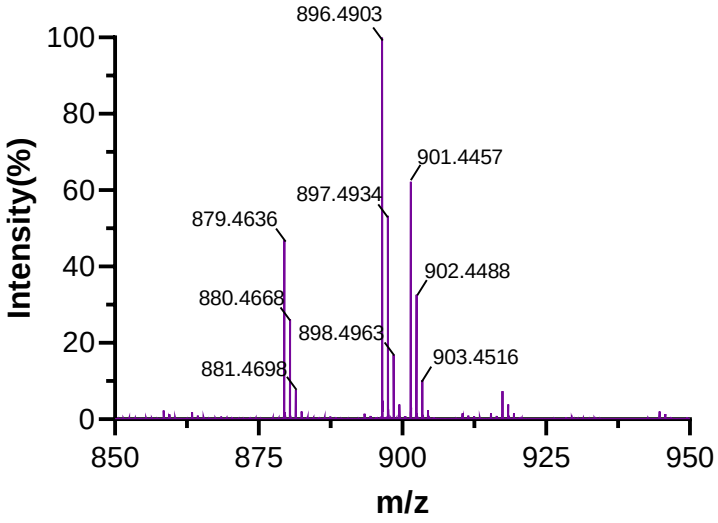

Probe 2: HR-MS (positive mode): calculated for $[M+H]^+$ 628.3691; $[M+Na]^+$ 650.3511; Found $[M+H]^+$ 628.3685; $[M+Na]^+$ 650.3504.

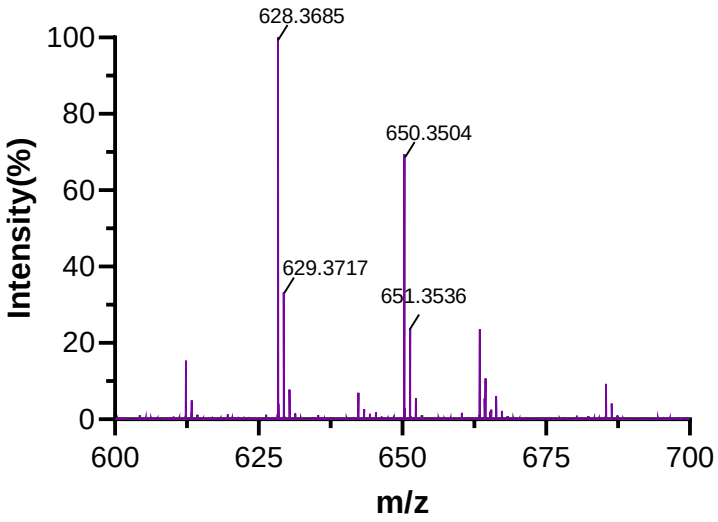

Supplementary Tables

Table S1. Photo-affinity-labeled proteins (Spot number 1 and 2 in Fig. S5) identified by 2-DE and MALDI-TOF/TOF MS. Human Fatty Acid Binding Protein 1 (FABP1) was identified.

Spot Number	Protein names	Accession No.	Protein Score	Protein Score C.I.%	Total ion score	Pep. count	Protein MW
1	Fatty acid binding protein 1	NP_001434.1	70	96.7	54	3	14256.4
Peptide information							
Calculated Mass	Observed Mass	± Da	± ppm	Start Seq.	End Seq.	Sequence	Rank Result Type
1063.651	1063.5737	-0.0773	-73	91	99	LVTTFKNIK	Mascot
1102.574	1102.6331	0.0591	54	81	90	TVVQLEGDNK	Mascot
1102.574	1102.6331	0.0591	54	81	90	TVVQLEGDNK	Mascot
1210.7042	1210.762	0.0578	48	21	31	AIGLPEELIQK	Mascot

Spot Number	Protein names	Accession No.	Protein Score	Protein Score C.I.%	Total ion score	Pep. count	Protein MW
2	Fatty acid binding protein 1	NP_001434.1	73	98.3	61	2	14256.4
Peptide information							
Calculated Mass	Observed Mass	± Da	± ppm	Start Seq.	End Seq.	Sequence	Rank Result Type
1030.5527	1030.5605	0.0078	8	37	46	GVSEIVQNGK	Mascot
1102.574	1102.6238	0.0498	45	81	90	TVVQLEGDNK	Mascot
1102.574	1102.6238	0.0498	45	81	90	TVVQLEGDNK	Mascot

References

1 Y. Liu, V. K. W. Wong, B. C. B. Ko, M. K. Wong and C. M. Che, *Org. Lett.* 2005, **7**, 1561-1564.

2 V. Vendrell-Criado, G. M. Rodríguez-Muñiz, M. Yamaji, V. Lhiaubet-Vallet, M. C. Cuquerella, M. A. Miranda. *J Am Chem Soc*. 2013,**135**, 16714-16719.

3 D. Hu, Y. Liu, Y. T. Lai, K. C. Tong, Y. M. Fung, C. N. Lok and C. M. Che, *Angew. Chem. Int. Ed. Engl.* 2016, **55**, 1387-1391.

4 T. Velkov, S. Chuang, R. Prankerd, H. Sakellaris, C. J. Porter and M. J. Scanlon, *Protein Expr. Purif.* 2005, **44**, 23-31.

5 J. Li, C. Yu, R. Wang, J. Xu, Y. Chi, J. Qin and Q. Liu, *Int. J. Biochem. Cell Biol.*, 2017, **90**, 121-135.

6 G. W. T. M. J. Frisch, H. B. Schlegel, G. E. Scuseria, M. A. Robb, J. R. Cheeseman, G. Scalmani, V. Barone, G. A. Petersson, H. Nakatsuji, X. Li, M. Caricato, A. Marenich, J. Bloino, B. G. Janesko, R. Gomperts, B. Mennucci, H. P. Hratchian, J. V. Ortiz, A. F. Izmaylov, J. L. Sonnenberg, D. Williams-Young, F. Ding, F. Lipparini, F. Egidi, J. Goings, B. Peng, A. Petrone, T. Henderson, D. Ranasinghe, V. G. Zakrzewski, J. Gao, N. Rega, G. Zheng, W. Liang, M. Hada, M. Ehara, K. Toyota, R. Fukuda, J. Hasegawa, M. Ishida, T. Nakajima, Y. Honda, O. Kitao, H. Nakai, T. Vreven, K. Throssell, J. A. Montgomery, Jr., J. E. Peralta, F. Ogliaro, M. Bearpark, J. J. Heyd, E. Brothers, K. N. Kudin, V. N. Staroverov, T. Keith, R. Kobayashi, J. Normand, K. Raghavachari, A. Rendell, J. C. Burant, S. S. Iyengar, J. Tomasi, M. Cossi, J. M. Millam, M. Klene, C. Adamo, R. Cammi, J. W. Ochterski, R. L. Martin, K. Morokuma, O. Farkas, J. B. Foresman and D. J. Fox., 2016.

7 R. M. B. D.A. Case, D.S. Cerutti, T.E. Cheatham, III, T.A. Darden, R.E. Duke, T.J. Giese, H. Gohlke, A.W. Goetz, N. Homeyer, S. Izadi, P. Janowski, J. Kaus, A. Kovalenko, T.S. Lee, S. LeGrand, P. Li, C. Lin, T. Luchko, R. Luo, B. Madej, D. Mermelstein, K.M. Merz, G. Monard, H. Nguyen, H.T. Nguyen, I. Omelyan, A. Onufriev, D.R. Roe, A. Roitberg, C. Sagui, C.L. Simmerling, W.M. Botello-Smith, J. Swails, R.C. Walker, J. Wang, R.M. Wolf, X. Wu, L. Xiao and P.A. Kollman University of California, San Francisco, 2016.

8 C. I. Bayly, P. Cieplak, W. D. Cornell and P. A. Kollman, J *Phys Chem-Us* 1993, **97**, 10269-10280.

9 J. Wang, R. M. Wolf, J. W. Caldwell, P. A. Kollman and D. A. Case, *J Comput Chem* 2004, **25**, 1157-1174.

10 G. M. Morris, R. Huey, W. Lindstrom, M. F. Sanner, R. K. Belew, D. S. Goodsell and A. J. Olson, *J Comput Chem* 2009, **30**, 2785-2791.

11 J. Cai, C. Lucke, Z. Chen, Y. Qiao, E. Klimtchuk and J. A. Hamilton, *Biophys J* 2012, **102**, 2585-2594.

12 B. Hess, C. Kutzner, D. van der Spoel, E. Lindahl and J. Chem. *Theory Comput.* 2008, **4**, 435-447.

13 S. Pall, M. J. Abraham, C. Kutzner, B. Hess and E. Lindahl, *Lect Notes Comput Sc* 2015, **8759**, 3-27.

14 K. Lindorff-Larsen, S. Piana, K. Palmo, P. Maragakis, J. L. Klepeis, R. O. Dror and D. E. Shaw, *Proteins* 2010, **78**, 1950-1958.

15 G. Bussi, D. Donadio and M. Parrinello, *J Chem Phys* 2007, **126**.

16 M. Parrinello and A. Rahman, *J Appl Phys* 1981, **52**, 7182-7190.

17 G. M. Morris, D. S. Goodsell, R. S. Halliday, R. Huey, W. E. Hart, R. K. Belew and A. J. Olson, *J Comput Chem,* 1998, **19**, 1639-1662.